

# Redistribution of adhering junctions in human endometrial epithelial cells during the implantation window of the menstrual cycle

Volker U. Buck · Reinhard Windoffer ·  
Rudolf E. Leube · Irmgard Classen-Linke

Accepted: 29 January 2012 / Published online: 12 February 2012  
© Springer-Verlag 2012

**Abstract** The human uterine epithelium is characterised by remarkable plasticity with cyclic changes in differentiation that are controlled by ovarian steroid hormones to optimise conditions for embryo implantation. To understand whether and how cell–cell adhesion is affected, the localisation of junction proteins was studied throughout the menstrual cycle. Expression patterns were examined by immunofluorescence in 36 human endometrial specimens of different cycle stages. Antibodies against the desmosomal proteins desmoplakin 1/2 (Dp 1/2) and desmoglein 2 (Dsg 2), the adherens junction proteins E-cadherin and  $\beta$ -catenin and also the common junctional linker protein plakoglobin showed a strong subapical staining during the proliferative phase until the early luteal phase (day 20). In the mid- to late luteal phase, however, these junctional proteins redistributed over the entire lateral plasma membranes. In contrast, tight junction proteins (ZO-1, claudin 4) remained at their characteristic subapical position throughout the menstrual cycle. mRNA levels of Dp 1/2, E-cadherin and ZO-1 obtained by real time RT-PCR were not significantly changed during the menstrual cycle. The observed redistribution of desmosomes and adherens junctions coincides with the onset of the so called implantation window of human endometrium. We propose

that this change is controlled by ovarian steroids and prepares the endometrium for successful trophoblast invasion.

**Keywords** Desmosome · Adherens junction · Tight junction · Human endometrium · Menstrual cycle · Implantation

## Introduction

The uterine surface epithelium and the endometrial glands are the first contact sites for the trophoblast. They play a key role in preparing and supporting early pregnancy. The adhesion and invasion of the trophoblast and final implantation of the blastocyst via the endometrial epithelium which normally behaves as a barrier is an unusual cell biological phenomenon involving substantial remodelling of the polarised endometrial epithelial cells (Denker 1993, 1994). In this functional context, the steroid hormone-controlled uterine epithelium presents a special case, since other simple epithelia such as the gastrointestinal mucosa do not undergo hormone dependent changes.

Endometrial epithelial cells display a typical polarised phenotype during the proliferative phase of the menstrual cycle (days 6–14), which is controlled by 17  $\beta$ -estradiol. The apical domain features a microvilli-rich brush border and is enriched in specific enzymes. During the luteal phase (days 15–28), which is predominantly governed by progesterone, the epithelial cells become ‘receptive’ for implantation (Denker 1993, 1994). Specialised apical protrusions termed pinopodes appear (Martel et al. 1981; Nikas et al. 1995) and changes in apical marker enzymes occur (Suzuki et al. 1981; Imai et al. 1992). Furthermore, epithelial cell morphology changes from a columnar to a more cuboidal type and glycogen vacuoles become visible.

**Electronic supplementary material** The online version of this article (doi:10.1007/s00418-012-0929-0) contains supplementary material, which is available to authorized users.

V. U. Buck · R. Windoffer · R. E. Leube · I. Classen-Linke (✉)  
Institute of Molecular and Cellular Anatomy,  
Medical Faculty, RWTH Aachen University,  
Wendlingweg 2, 52074 Aachen, Germany  
e-mail: iclassen-linke@ukaachen.de  
URL: <http://www.moca.rwth-aachen.de>

In addition to these cyclic epithelial cell alterations pronounced changes occur in the basal lamina. Expressions of the basal lamina components laminin and type IV collagen are altered periodically in relation to the menstrual cycle (Aplin et al. 1988; Bilalis et al. 1996; Tanaka et al. 2009).

These alterations of morphology and composition of apical and basal domains are likely associated with changes in cell–cell adhesion, which, however, has not been studied adequately to date. Using specific and well-characterised immunological reagents we therefore systematically examined the cycle-dependent distribution of the three major junctions, which together form the tripartite junctional complex at the subapical circumference of polarized epithelia (Farquhar and Palade 1963). It consists of the intermediate keratin filament-anchoring desmosomes (maculae adhaerentes) at the bottom, the actin-associated belt-like adherens/intermediate junctions (zonulae adhaerentes) in the middle and the adluminal tight junctions (zonulae occludentes), which are responsible for maintaining overall polarity by separating the apical from the basolateral domain. The aim of the study was to investigate whether and how these junctions are affected in human endometrial epithelial cells during the menstrual cycle.

## Materials and methods

### Human tissue samples

Endometrial tissue samples were obtained from fertile women, aged 25–52 (mean 41.8 years) undergoing hysterectomy due to benign uterine diseases. Samples were collected in the Departments of Gynecology and Obstetrics of the St. Antonius Hospital in Eschweiler, the Luisenhospital and Marienhospital in Aachen and at the University Hospital of RWTH Aachen University. The use of the tissues was approved by the Ethics Committee of the Medical Faculty of the University of Aachen (EK 347). All patients had a regular menstrual cycle and did not receive hormonal treatment for at least 3 months before surgery. Dating of each specimen was done by menstrual history and histological examination according to the criteria of Noyes et al. (1950). Some specimens could not exactly be determined on one single day, but only with an accuracy of 2–4 days (e.g. ‘18/19’ or ‘4–7’, respectively). For immunohistochemistry, uterine tissue was frozen in liquid nitrogen immediately after hysterectomy and stored at  $-40^{\circ}\text{C}$  until further processing. Thirty-six endometrial specimens were obtained at the following days of the menstrual cycle: one at days 6, 7, 8 each; three at day 9; one at days 10, 11, 13/14 each; four at day 14; two at day 17; two at day 17/18; two at day 18; one at day 18/19; three

at day 19; two at day 20/21; one at days 21, 21/22, 22/23, 23 each; three at day 24; one at day 25/26; two at day 26; one at day 27. They were grouped into *proliferative phase* (days 6–14,  $n = 13$ ), *early luteal phase* (days 15–19,  $n = 10$ ), *mid-luteal phase* (days 20–23,  $n = 6$ ) and *late luteal phase* (days 24–28,  $n = 7$ ). From each specimen at least three sections were stained. For real time RT-PCR, uterine tissue was directly transferred into RNeasy<sup>®</sup> (Ambion, Huntingdon, United Kingdom) and stored at  $-40^{\circ}\text{C}$  until further processing. Real time RT-PCR was done on 23 samples of the following cycle days: one at day 6; three at day 4–7; three at day 7; one at days 8, 9, 10, 11–14 each; two at day 14; one at days 17, 18 each; two at day 19; two at day 20; one at day 23; two at day 24; one at day 26.

### Immunohistochemistry

Detailed information on all antibodies and sera is provided in Table 1. Immunofluorescence staining was performed on 8 to 10- $\mu\text{m}$  thick cryostat sections mounted on SuperFrost<sup>®</sup> plus glass slides (Thermo Fisher Scientific/Bonn, Germany). Sections were fixed in acetone for 10 min at  $4^{\circ}\text{C}$ , air dried and stored at  $-20^{\circ}\text{C}$ . Slides were rehydrated in PBS for 10 min and blocked for 20 min with 5% goat and/or donkey serum (Table 1), respectively. Antibodies were diluted with PBS supplemented with 1.5% bovine serum albumin. After overnight incubation at  $4^{\circ}\text{C}$  with primary antibodies, slides were rinsed in PBS three times and then incubated for 1 h in the dark at room temperature with secondary antibodies (Table 1). For immunofluorescent double labeling both primary antibodies were applied together. Similarly, both secondary antibodies were mixed in the next incubation step. Slides were counterstained with 4',6-diamidino-2-phenylindole, dihydrochloride (DAPI 1  $\mu\text{g}/\text{ml}$ , Sigma/Hamburg, Germany) for 30 min at room temperature. Slides were then rinsed again in PBS three times and washed in deionised water. Sections were mounted with Kaiser's glycerol gelatin (Merck/Darmstadt, Germany) and stored at  $4^{\circ}\text{C}$  until microscopical assessment. For controls, the specific primary antibodies were either omitted or replaced by normal mouse or rabbit IgG with the same protein content as the primary antibody. No specific staining of these negative controls was observed.

### Microscopical analysis

Sections were assessed and scanned with a confocal laser scanning microscope (LSM 710 Duo, Zeiss/Jena, Germany) and evaluated using the ZEN 2009 software (Zeiss/Jena, Germany). Epifluorescent and differential interference contrast (DIC) images were taken by an Axio Imager M.2 microscope with an ApoTome.2 unit using an

**Table 1** Reagents for immunohistochemistry

	Antigen/serum	Host (isotype)	Clone (Cat. No.)	Source	Dilution
Primary antibodies	Desmoplakin 1/2	Mouse (IgG)	2.15/2.17/2.20	Progen Biotechnik, Heidelberg, Germany	1:10
	Desmoglein 2	Rabbit polyclonal	–	kind gift of Dr. Bastian Holthöfer, Mainz (Schlegel et al. 2010)	1:1,000
	Plakoglobin ( $\gamma$ -catenin)	Goat polyclonal	(# sc-30997)	Santa Cruz Biotechnology, Santa Cruz, CA	1:100
	$\beta$ -Catenin	Rabbit polyclonal	(# C 2206)	Sigma-Aldrich, Saint Louis, Missouri	1:2,000
	E-Cadherin	Mouse (IgG 1)	5H9	Progen Biotechnik, Heidelberg, Germany	1:10
	ZO-1	Rabbit polyclonal	(# 40-2200)	Invitrogen, Carmarilla, CA	1:100
	Claudin 4	Rabbit polyclonal	(# RB-9266-P0)	Thermo Fisher Scientific, Fremont, CA	1:50
Secondary antibodies	Alexa Fluor 488 goat anti mouse	Goat (IgG H + L)	(# A11017)	Invitrogen, Eugene, USA	1:500
	Cy 2 goat anti mouse	Goat (IgG H + L) F(ab') <sub>2</sub>	(# 610-111-121)	Rockland, Gilbertsville, PA	1:100
	Cy 3 donkey anti rabbit	Donkey (IgG H + L) F(ab') <sub>2</sub>	(# 711-166-152)	Jackson, West Grove, USA	1:1,000
	Mouse negative control	Mouse (IgG 1)	(# X 0931)	Dako, Glostrup, Denmark	3 $\mu$ g/ml
	Rabbit negative control	Rabbit (IgG fraction)	(# X 0936)	Dako, Glostrup, Denmark	3 $\mu$ g/ml
	Goat serum/blocking reagent	Goat	(# sc-2043)	Santa Cruz Biotechnology, Santa Cruz, CA	1:20
	Donkey serum/blocking reagent	Donkey	(# sc-2044)	Santa Cruz Biotechnology, Santa Cruz, CA	1:20

Axiocam MRm camera. Pictures were evaluated with the AxioVision software (version 4.8, Zeiss/Jena, Germany). Processing of exported z-stack slices for 3-D animation was performed by use of the image processing program FIJI based on ImageJ.

#### Real time RT-PCR (Light cycler)

Total RNA was isolated from endometrial samples using the High Pure RNA Tissue Kit (Roche, Mannheim, Germany). Endometrial tissue (25 mg) was transferred to 900  $\mu$ l lysis-/binding-buffer and was homogenised for 90 s with a glass-Teflon-homogeniser. Thereafter, 700  $\mu$ l of a water-saturated phenol/chloroform/isoamyl alcohol mix (Ambion, Huntingdon, United Kingdom) was added, mixed and subjected to centrifugation (13,000g, 2 min, room temperature). The supernatant was mixed with 0.5 volumes of ethanol and loaded onto the column provided with the kit. The following steps of RNA isolation were done according to the kit protocol with minor modifications: (a) DNase I treatment was prolonged to 30 min and was performed at room temperature, and (b) the RNA was eluted using two times 50  $\mu$ l of elution buffer.

Before performing PCR, RNA integrity numbers (RIN) were controlled for each mRNA sample to determine the degree of mRNA quality (Schroeder et al. 2006). RIN

values were measured at the IZKF Chip Facility of RWTH Aachen University (using an Agilent 2100 bioanalyzer system) and revealed a mean of 7.3 (SEM 0.759).

Total RNA (1  $\mu$ g) was reverse transcribed into cDNA using oligo-(dT)<sub>15</sub> primer and the 1st strand cDNA synthesis (AMV) Kit (Roche, Mannheim, Germany). Real time-PCR was performed with the Light Cycler (Roche, Mannheim, Germany) for Dp 1/2, E-cadherin, ZO-1, Cytokeratin 18 (CK 18) and Vimentin, respectively. 5-Aminolevulinat-synthetase 1 (ALAS1), which is expressed with ~500 mRNA molecules/cell, was used as reference gene. For amplification of the different cDNAs, the TaqMan Master Kit was used. Forward and reverse primers and corresponding TaqMan probes were selected with the help of the Universal ProbeLibrary (UPL) Assay Design Center (Roche). The primer pairs and UPL probes are listed in Table 2. The PCR runs were programmed with the Light Cycler Software Version 3.5. The runs included the following three steps: (1) Denaturation and activation of the Taq-Polymerase at 95°C, 10 min. (2) Amplification and quantification: denaturation at 95°C for 10 s; annealing at 60°C for 30 s, extension at 72°C for 1 s. (3) Cooling to 40°C for 30 s. The PCR volume was 20  $\mu$ l and consisted of 2  $\mu$ l cDNA and 18  $\mu$ l PCR reaction mix. The MgCl<sub>2</sub> concentration was 3 mM. Water was used as negative control in each PCR reaction. To determine the PCR efficiencies for

**Table 2** Primer sequences and UPL probes for real time RT-PCR

Name	Sequence (5'–3')	Roche UPL probe
ALAS-1 f	ACGCAGTGGGGCTTTATG	58
ALAS-1 r	ACCCTCCAACACAACCAAAG	58
Desmoplakin 1/2 f	GAAATATCTGGCAAACGAGACA	6
Desmoplakin 1/2 r	GCCAGCTGGAGCTCATAATC	6
E-cadherin f	CAGGCTCAAGCTATCCTTGC	75
E-cadherin r	AGTCATGCGTAGTGGTGCAT	75
ZO-1 f	AGGTGAAACACTGCTGAGTCC	9
ZO-1 r	TTTGCCAGGTTTTAGGATCAC	9
Cytokeratin 18 f	TGATGACACCAATATCACACGA	63
Cytokeratin 18 r	CTGGGCTTGTAGGCCTTTTA	63
Vimentin f	AGGTGGACCAGCTAACCAAC	63
Vimentin r	TTCGGCTTCCTCTCTGAA	63

quantitative mRNA assessment, coefficient files were created for the ALAS1-PCR reaction and the mRNA amplicates of interest. The slope of the ALAS1-PCR was  $-3,282$ . The slopes for the Dp 1/2-, E-cadherin-, ZO-1-, CK 18- and Vimentin-PCR were  $-3,556$ ,  $-3,403$ ,  $-3,460$ ,  $-3,393$  and  $-3,530$ , respectively. The final quantitative analysis of the PCR reactions was accomplished with the RelQuant Software, Version 1.01 (Roche) with the use of the different coefficient files in comparison with the ALAS1 coefficient files. Results are shown as 'relative units'.

## Results

Desmosomal proteins are redistributed over the entire lateral membrane during the mid to late luteal phase in the functionalis layer

To detect desmosomes, antibodies directed against the cytoplasmic plaque proteins desmoplakin 1 and 2 (Dp 1/2) and the transmembrane cadherin desmoglein 2 (Dsg 2) were used. They showed a distinct multipunctate staining pattern at the lateral membranes of endometrial epithelial cells representing single desmosomes (Figs. 1, 2, 3). During the proliferative phase (days 6–14), the spot-like staining was most prominent near the apical pole of the lateral cell membrane with only a few desmosomes along the lateral plasma membrane (Figs. 1, 3). The subapical enrichment even increased somewhat in the early to mid-luteal phase until day 20 (Figs. 1c, 3c). This subapical fluorescence pattern was found consistently in the stratum basale in all samples irrespective of the cycle stage (Fig. 2a, c). In contrast, the glands within the functionalis layer of the endometrium presented characteristic changes

in distribution (Fig. 2a, b). During the mid- to late luteal phase, desmosomes became evenly distributed along the entire lateral plasma membranes (Figs. 1, 3e, g). Some of the images suggested apical and/or basal localisation of desmoplakin-positive puncta (e.g. arrowheads in Fig. 1e, g). 3D reconstructions of the recorded fluorescence were therefore prepared. The resulting animations provided as supplementary material (Online Resource 1) showed, however, that the observed redistribution of desmosomal proteins is restricted to the lateral plasma membrane domain and does not include the apical or basal domains.

Adherens junction proteins redistribute from a belt-like subapical zone to lateral puncta during the luteal phase in the functionalis layer

The transmembrane protein E-cadherin and the intracellular anchor protein  $\beta$ -catenin were immunolocalised as markers of adherens junctions. They are enriched subapically surrounding the cell apex as continuous circumferential belts. This subapical staining pattern was observed in the basalis layer throughout the menstrual cycle (not shown). Pronounced changes, however, were noted again in the functionalis layer. While strong staining intensity was observed in the subapical region of the lateral plasma membranes during the late proliferative to early luteal phase (Figs. 4b, c, 5a, b), this subapical maximum disappeared during the mid-luteal phase and was not detectable any more during the late luteal phase (Figs. 4d, 5c, d).

Plakoglobin reflects cyclic changes of both types of adhering junctions

In the next set of experiments, the distribution of the intracellular linker protein plakoglobin ( $\gamma$ -catenin) was examined. This protein is present in adherens junctions and also in desmosomes (Cowin et al. 1986; Holthofer et al. 2007; Garrod and Chidgey 2008). As expected, the staining changed in the stratum functionale as described before for the specific desmosomal and adherens junction markers during the menstrual cycle (Fig. 6).

The distribution of tight junction proteins is not affected by the menstrual cycle

The staining of antibodies directed against the tight junction protein zonula occludens protein 1 (ZO-1) was studied next. Endometrial epithelial and endothelial cells presented a distinct lateral staining that is typical for tight junctions (Fig. 7). Confocal scans of double-label immunofluorescence revealed that the ZO-1-positive tight junctions localised at the most apical lateral plasma membranes above desmoplakin-positive desmosomes (Fig. 8). In

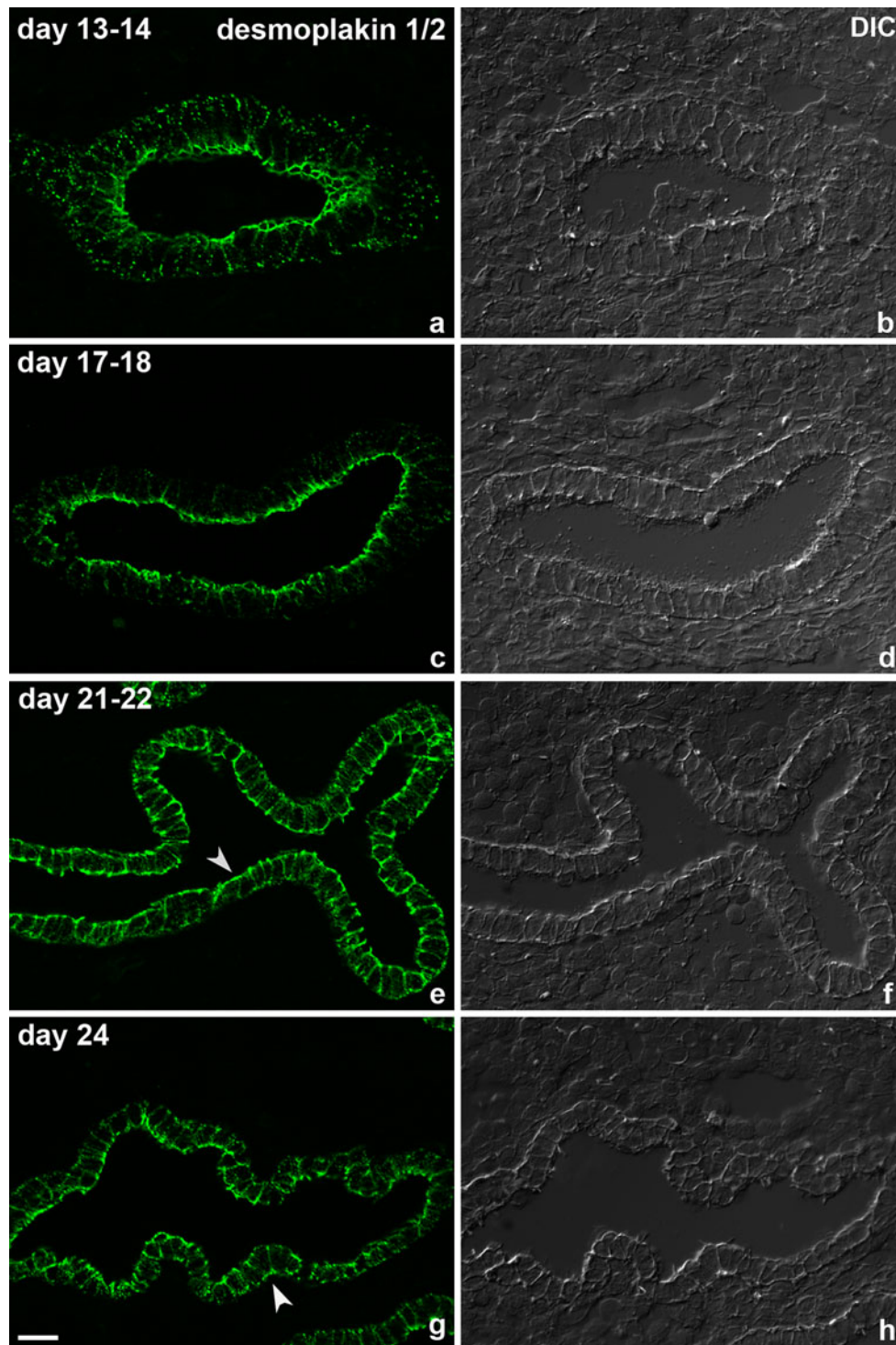


**Fig. 1** Immunostaining of *desmoplakin* (Dp) 1/2 on glandular endometrial epithelial cells at different times of the menstrual cycle (**a, c, e, g**). Corresponding differential interference contrast (DIC) images of the same slices in **b, d, f** and **h**. Note the subapical enrichment of immunoreactivity at days 13–14 and 17–18 that is lost

around day 20 with Dp 1/2 staining along the entire lateral plasma membrane. Days of the menstrual cycle are indicated on the left. *Arrowhead* in **e** points to the apical membrane; *arrowhead* in **g** points to the basal membrane. Apotome images. *Scale bar* 20  $\mu\text{m}$

contrast to the cycle-dependent redistribution of adherens junctions and desmosomes, ZO-1 did not show any detectable change in its localisation during the menstrual

cycle (Figs. 7, 8). These results are further supported by immunofluorescence analyses using antibodies directed against the transmembrane protein claudin 4, which is also

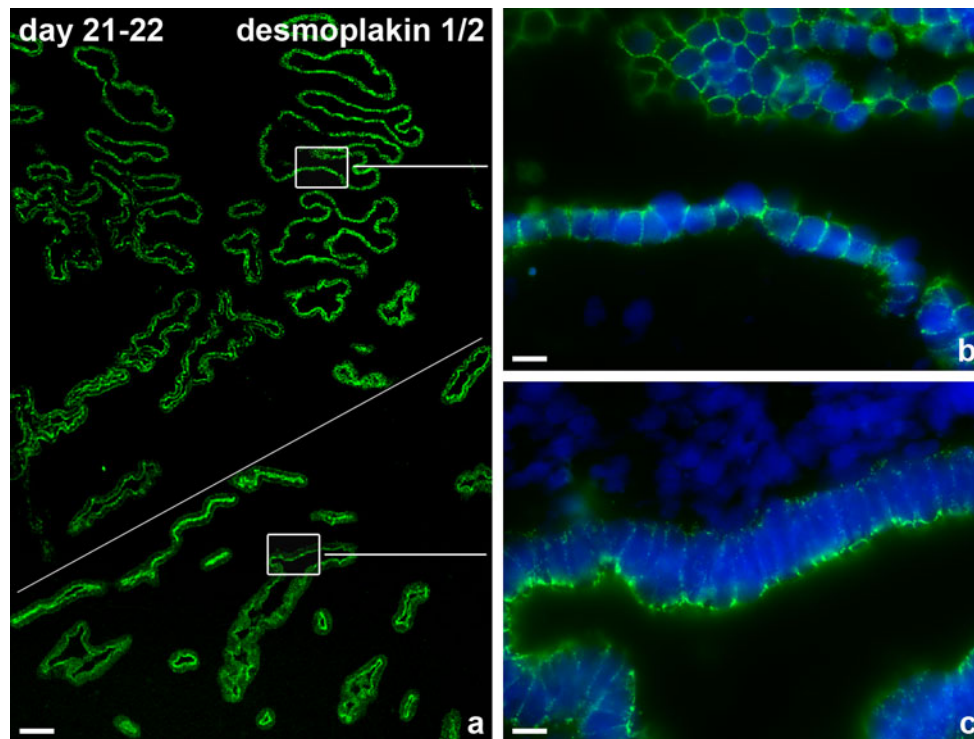


**Fig. 2** Cross section through an endometrial specimen at day 21–22 of the menstrual cycle stained for *desmoplakin* (Dp) 1/2. The *diagonal line* (a) separates the upper functionalis from the lower basalis layer. Redistribution along the lateral plasma membranes occurs only in

glandular epithelial cells of the functionalis region, while the subapical staining persists in the basalis region (25-fold magnification in b and c combined with DAPI staining). Scale bars 250  $\mu\text{m}$  (a); 10  $\mu\text{m}$  (b, c)

specific for tight junctions. The subapical staining of the lateral plasma membranes was similar to that of ZO-1 and was not changed during the menstrual cycle (Online Resource 2).

mRNA levels of Dp1/2, E-cadherin and ZO-1 are not significantly changed during the menstrual cycle

Real time RT-PCR was performed to assess putative changes in the transcription of the genes coding for junction proteins. Several RT-PCR runs were performed with a total of 23 samples. Data of one representative RT-PCR run with samples throughout the menstrual cycle are shown in Fig. 9. A slight mRNA increase was observed for Dp1/2 and E-cadherin during the luteal phase (Fig. 9a, b). This may be due to the increased ratio of endometrial glands to stromal cells in the luteal phase. To prove this assumption, real time RT-PCRs were performed on the same mRNA samples with CK 18 as a marker for epithelial cells and Vimentin as a marker for stromal cells. The results are presented as relative units in the same graph in Fig. 9d revealing an inverse relationship with an increase of epithelial CK 18 cells and a decrease of stromal Vimentin cells in the luteal phase. These findings concluded that the changes are only due to a relative increase in the number of

epithelial cells but not to an increased expression per cell during the luteal phase of the menstrual cycle.

## Discussion

The importance of adhering junction redistribution for trophoblast invasion

The localisation of cell–cell adhesion molecules was analysed for the first time systematically in a large number of human endometrial samples throughout the menstrual cycle. We find that both types of adhering junctions are redistributed from the compact tripartite junctional complex to the entire lateral membrane domain of glandular epithelial cells during the mid- and late luteal phase whereas tight junctional components are not affected. Remarkably, the reorganisation of the adhering junctions is restricted to the functionalis layer, i.e. the part of the endometrium that facilitates embryo implantation. The receptive phase of the endometrium, referred to as the ‘implantation window’, lasts about 4 days (Bergh and Navot 1992) and coincides precisely with the observed junctional rearrangements. This suggests that the junctional redistribution prepares the endometrium for the invasion of

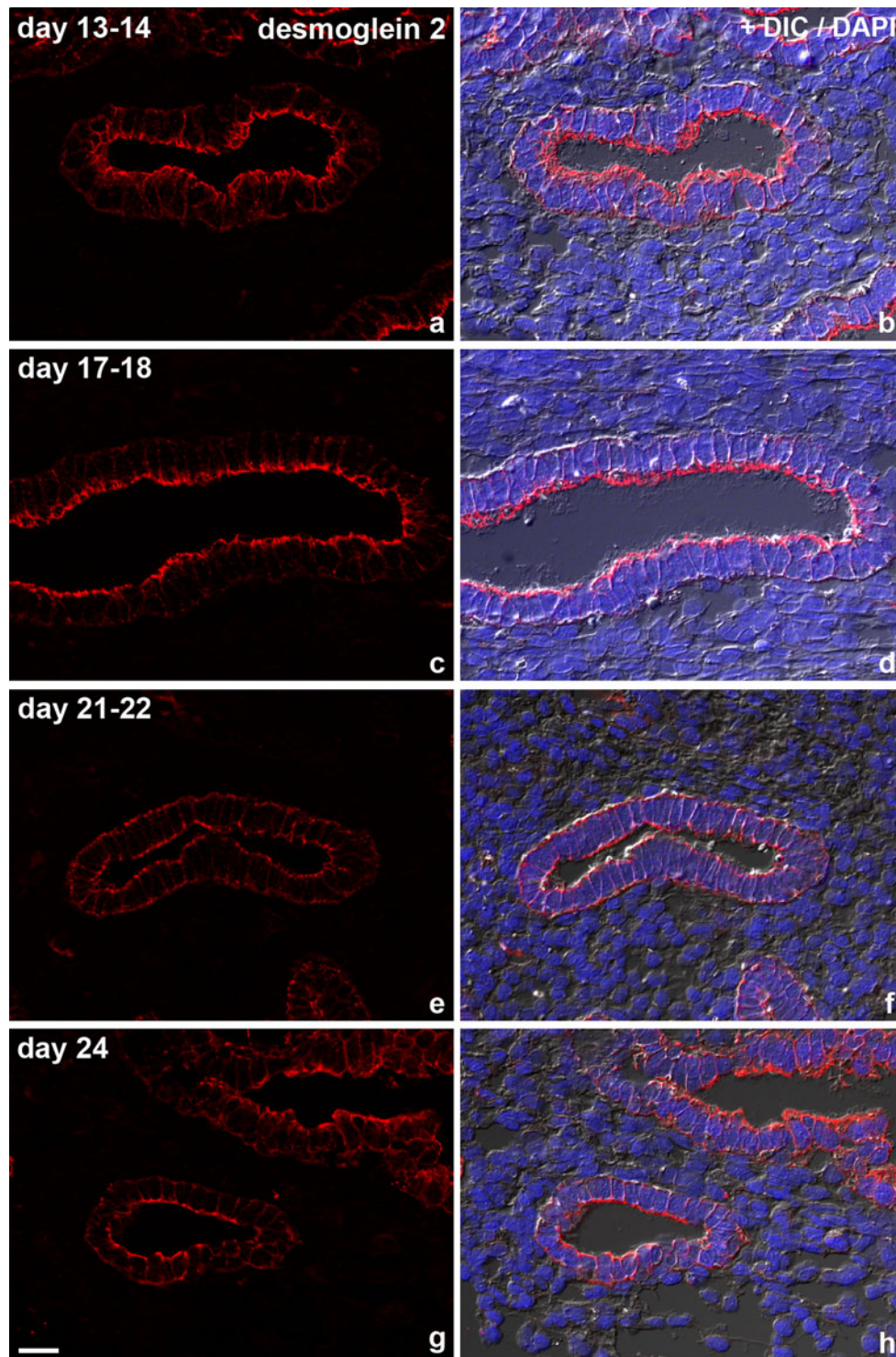


**Fig. 3** Immunostaining of *desmoglein* (Dsg) 2 on glandular endometrial epithelial cells at different times of the menstrual cycle (**a**, **c**, **e**, **g**). Merged with differential interference contrast (DIC) and DAPI

staining in **b**, **d**, **f** and **h**. Dsg 2 is localised and redistributed like Dp 1/2. Days of the menstrual cycle are indicated on the *left*. Apotome images. Scale bar 20  $\mu$ m

trophoblast cells. Thus, during the proliferative phase the barrier function of the epithelium is most important. It is supported by the compact and the tightly organised junctional complex, as it is typical for most simple epithelia. At

that time the endometrium is considered to be hostile towards embryo implantation (Kabir-Salmani et al. 2008). By breaking down the junctional complex during the luteal phase cell adhesion may be weakened. Concurrently,

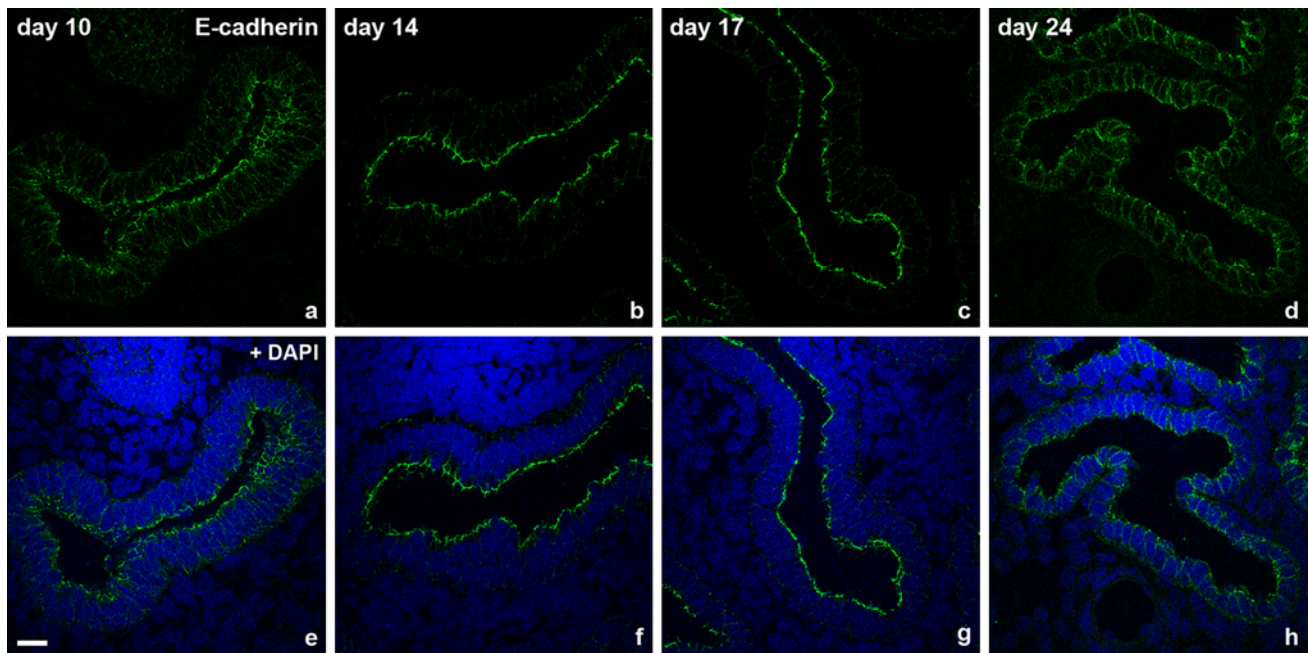


**Fig. 4** Immunostaining of *E-cadherin* on glandular endometrial epithelial cells at different times of the menstrual cycle (**a, b, c, d**). Merged with DAPI staining in **e, f, g** and **h**. *E-cadherin* is localised and redistributed along the lateral plasma membranes similar to the

desmosomal proteins. The staining against this adherens junction protein is less punctuated than the desmosomal staining (Figs. 1, 2, 3). Days of the menstrual cycle are indicated on the left. Confocal LSM images. Scale bar 20  $\mu$ m

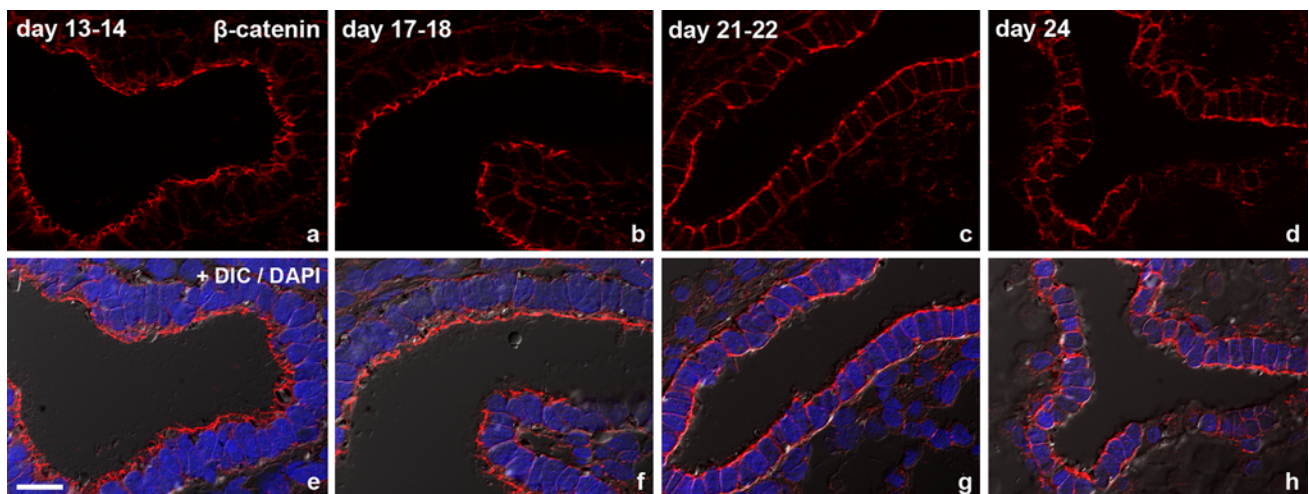


**Fig. 5** Immunostaining of  $\beta$ -catenin on glandular endometrial epithelial cells at different times of the menstrual cycle (**a, b, c, d**). Merged with differential interference contrast (DIC) and DAPI staining in **e, f, g** and **h**. The strong subapical staining is even more

pronounced than the anti-*E-cadherin* staining shown above. Days of the menstrual cycle are indicated on the left. Apotome images. Scale bar 20  $\mu$ m

cytoskeletal rearrangements are expected to occur that may further support the uptake of the trophoblast. In accordance, Morris et al. (2011) recently reported a redistribution of the actin-binding protein cofilin which is involved in the regulation of actin dynamics in cycling human endometrium. In the proliferative phase, cofilin was localised at the apical side of luminal epithelial cells, while

it was localised to the basolateral side during the luteal phase.

Recent studies on gland involvement during early pregnancy suggest an alternative route of invasion by the ‘glandular trophoblast’ (Moser et al. 2010). First trimester trophoblast cells were found in between glandular endometrial epithelial cells in explant confrontation assays.



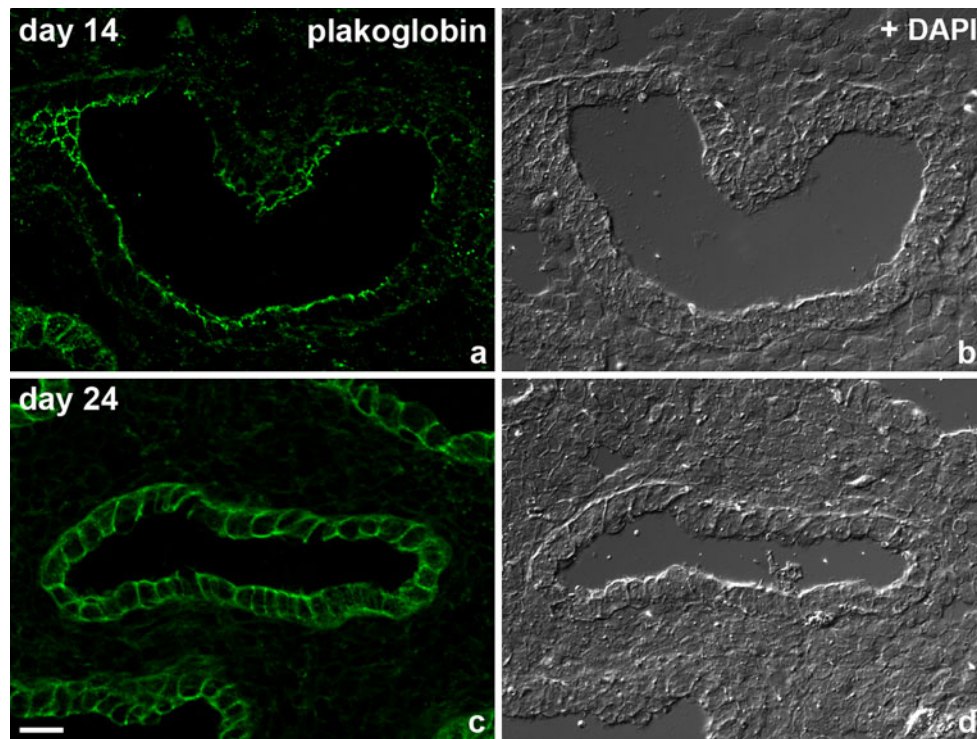


**Fig. 6** Immunostaining of *plakoglobin* on glandular endometrial epithelial cells of the proliferative phase (**a, b**) and of the luteal phase (**c, d**) of the menstrual cycle. Differential interference contrast (DIC) of the same slices in **b** and **d**. A subapical staining can be discerned in

the proliferative phase (day 14) and again, a staining of the whole lateral membrane in the luteal phase (day 24). Apotome images. Scale bar 20  $\mu$ m

Trophoblasts invaded the epithelial layer from the luminal/apical side and also from its basal margin. The redistribution of cell–cell adhesion proteins observed in our study would support trophoblast invasion by either route.

In general, there is increasing evidence for the plasticity of epithelial lateral cell–cell adhesion complexes in the literature. For example, Kametani and Takeichi (2007) described a lateral ‘cadherin-flow’ in vitro, implicating a possible functional significance for the sliding of two contacting cell membranes and Roberts et al. (2011) emphasised the importance of desmosome dynamics in migrating epithelial cells dependent on the actin cytoskeleton.

#### Menstrual cycle-dependent fluctuation in junction distribution and junctional protein expression in human endometrial cells

Our study extends previous observations on the expression of adherens and desmosomal junctions in human endometrium. In a morphometric study, using electron microscopy, the ratio of desmosomes to the cell surface of luminal epithelial cells was shown to be significantly reduced at day 6 after LH surge, the time of implantation (Sarani et al. 1999). Focusing on changes occurring during menstruation,

Tabibzadeh et al. (1995) reported a ‘disorganisation’ of the site-specific distribution of Dp 1/2, E-cadherin and  $\alpha$ - and  $\beta$ -catenin at menstruation, but no change at the other menstrual stages. The immunohistochemical ABC detection technique that was used in this study, however, is not suited to discern the different distribution patterns observed in our study using confocal microscopy and epifluorescence. Nei et al. (1996) studied the expression of Dp 1/2 and Dsg 2 in endometrial carcinoma in comparison to normal endometrium. They showed by confocal laser scanning semiquantification of fluorescence intensity that the expression of desmosomal proteins decreased in immunostained tissue sections of endometrial carcinoma with higher tumour grading and loss of differentiation. In normal endometria, however, no apparent difference in fluorescence intensity was observed throughout the cycle. Fujimoto et al. (1996) on the other hand, reported an upregulation of these proteins at the mRNA level in the luteal phase of the menstrual cycle. These results were obtained by semiquantitative Southern blot analysis of RT-PCR products obtained from homogenised endometrium. However, they may only reflect the relative increase of epithelial tissue in the luteal phase which we have also detected in our study. In accordance with this interpretation, Matsuzaki et al. (2010) could not detect any cyclic

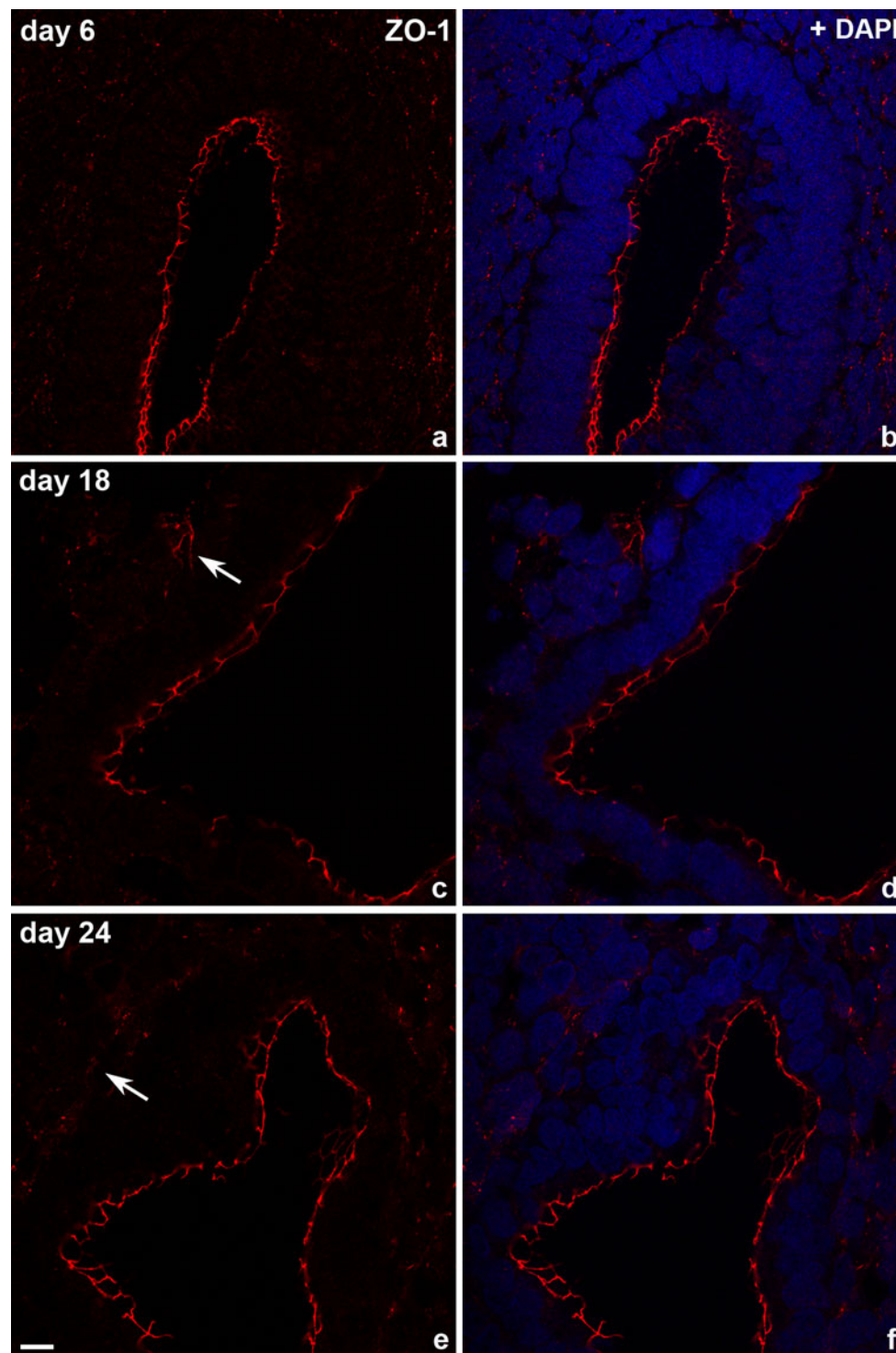


**Fig. 7** Immunostaining of *ZO-1* on glandular endometrial epithelial cells at different times of the menstrual cycle (**a**, **c**, **e**). Merged with DAPI staining in **b**, **d** and **f**. The tight junction protein *ZO-1* does not change in distribution or staining intensity during the cycle. It appears either as a ‘subapical ring’ or as a thin line in the most apical region of

mRNA changes of E-cadherin and  $\beta$ -catenin in microdissected glandular epithelial cells by quantitative real time RT-PCR.

the lateral plasma membranes. The *arrows* in **c** and **e** point at endothelial cells of endometrial vessels that are also stained by the anti-*ZO-1* antibody. Days of the menstrual cycle are indicated on the *left*. Confocal LSM images. *Scale bar* 10  $\mu$ m

Our data on the distribution of plakoglobin ( $\gamma$ -catenin), which is present in both, desmosomes and adherens junctions, further strengthen our findings that desmosomes and

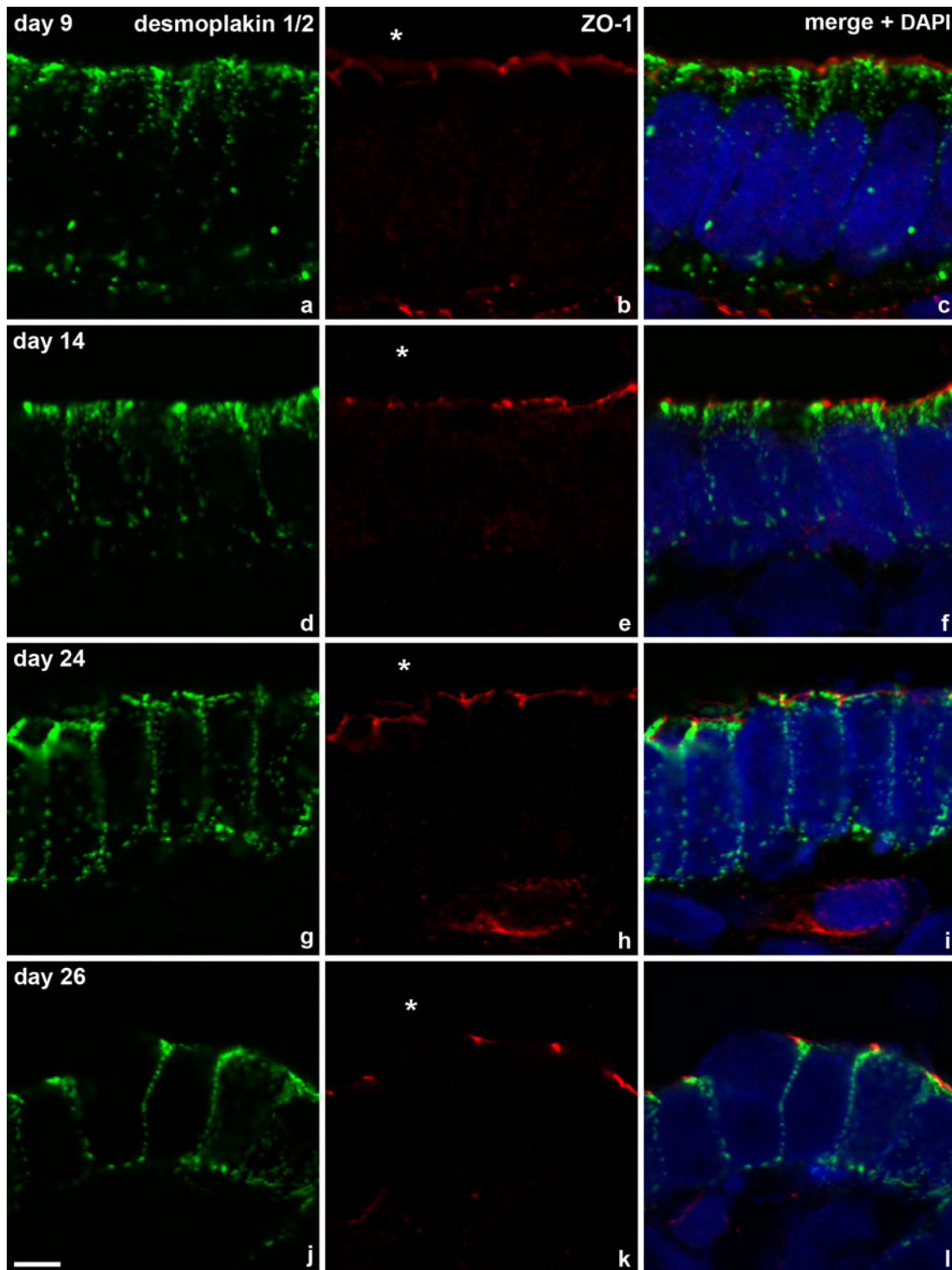
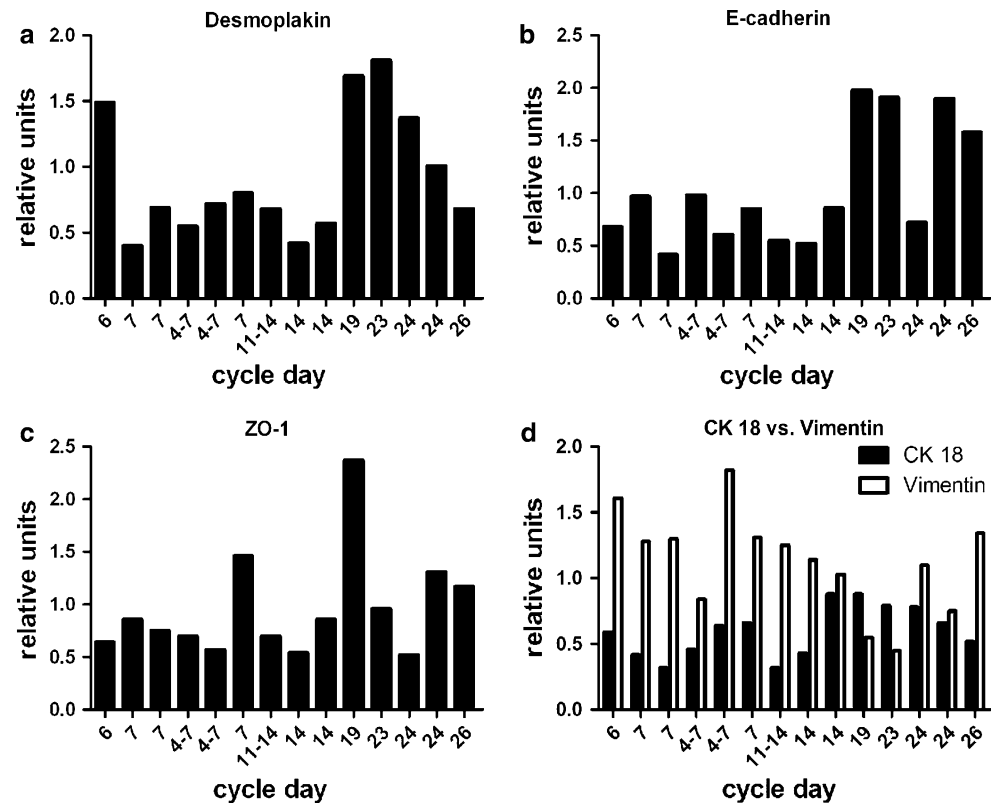


**Fig. 8** Double immunostaining of *desmoplakin* (Dp) 1/2 (**a, d, g, j**) and *ZO-1* (**b, e, h, k**) on glandular endometrial epithelial cells of the proliferative phase (day 9 and 14) and of the luteal phase (day 24 and 26). Merged pictures combined with DAPI staining in **c, f, i, and l**.

The tight junction protein *ZO-1* is clearly localised above Dp 1/2 staining in both phases of the menstrual cycle. The glandular lumen is marked by *asterisks* in **b, e, h** and **k**. Days of the menstrual cycle are indicated on the *left*. Confocal LSM images. *Scale bar* 5  $\mu$ m

**Fig. 9** Real time RT-PCR performed on specimens at different times of the menstrual cycle. Data are shown for 14 representative samples of one RT-PCR run;  $n = 1$ . Ratios of CK 18 to Vimentin account for the increase of Dp1/2 and E-cadherin mRNA levels in the luteal phase: a relatively high Dp 1/2 mRNA level (e.g. at day 19 and 23) (a), correlates with a high ratio of CK 18 to Vimentin in the respective specimens (d); low Dp 1/2 mRNA (e.g. day 26) (a), on the other hand, corresponds to a higher level of Vimentin mRNA in comparison to CK 18 mRNA. Accordingly, no significant change in mRNA expression during the menstrual cycle could be detected for Dp 1/2, E-cadherin or ZO-1



adherens junctions are rearranged in a similar fashion. A change in distribution of E-cadherin/plakoglobin could also be observed in the adhesive RL-95-2 endometrial carcinoma cell line. In contrast, the non-adhesive HEC-1-A cell line exhibited the pattern of typical polarised cells concentrating junctional proteins in a subapical belt (Thie et al. 1996).

Interestingly, the hypothesis that a change in cell–cell adhesion complexes facilitates implantation in humans has originally been deduced from changes of tight junctions during the human menstrual cycle as observed by freeze-fracture electron microscopy (Murphy et al. 1982, 1992). These studies revealed changes in the complexity of tight junctions when comparing specimens from the late proliferative/early luteal phase (days 14–16) with the mid- to late luteal phase (days 24–25). Tight junctions of luminal epithelial cells of late luteal phase did not extend as far down the lateral membrane (0.21  $\mu\text{m}$ ) as tight junctions from the late proliferative/early luteal phase of the menstrual cycle (0.43  $\mu\text{m}$ ). Such changes could not be resolved in our study which was based on light microscopic evaluation of immunofluorescent staining patterns of the tight junction proteins ZO-1 and claudin 4 during the menstrual cycle.

#### Species-specific similarities and differences of menstrual cycle-dependent adhesion

Studies on early implantation in different species revealed changes in desmosomal cell–cell adhesion between

endometrial epithelial cells which was proposed to lead to a facilitation of trophoblast invasion. Rabbit uterine epithelial cells showed a strong subapical staining of Dp 1/2 in the preimplantation phase. In the implantation phase, the desmosomal plaque proteins were evenly distributed throughout the entire lateral plasma membrane (Classen-Linke and Denker 1990). Illingworth et al. (2000) found a reduction of desmosomes in the mouse uterine luminal epithelium during the preimplantation phase of pregnancy. From days 1 to 5 of pregnancy, Dp 1/2 mRNA and protein levels decreased and a loss of desmosomes was observed by electron microscopy. A loss of desmosomes during early pregnancy was also found in rat uterine epithelial cells (Preston et al. 2004, 2006) by immunostaining against Dsgs and ultrastructural analyses. In addition, Preston et al. (2004) observed a different distribution of Dsgs at various stages of pregnancy. On day 1 of pregnancy, when oestrogen levels are high, a staining along the full length of the lateral plasma membrane was detected. By days 6 and 7 of pregnancy or by progesterone treatment of ovariectomised rats Dsg immunofluorescence was almost exclusively located at the apical part of the lateral membrane. This is in contrast to the observed redistribution during rabbit implantation (Classen-Linke and Denker 1990; Denker 1993) and the findings of this study. These differences may be due to species-specific differences of trophoblast–uterine interaction (Schlafke and Enders 1975). While for mice and rats the displacement type of implantation has been

described, in which whole groups of uterine epithelial cells detach from their basement membrane, rabbits display a fusion type of implantation by which syncytiotrophoblasts and uterine epithelial cells fuse to form a mixed syncytium. This might also explain the freeze-fracture results of Winterhager and Kuhnel (1982) on pseudopregnant rabbit uteri. In contrast to the previously discussed results on cycling human endometrium (Murphy et al. 1982, 1992), they showed an extension of tight junctions during the preimplantation phase. The implantation mode in humans is assumed to be of the intrusion type, in which the trophoblast cells penetrate between uterine epithelial cells breaking open the intercellular junctions and forming new junctions with the uterine epithelium and among each other. Data from *in vitro* studies support this assumption. Using transmission electron microscopy, Bentin-Ley et al. (2000) reported that trophoblast cells of human blastocysts from *in vitro* fertilisation treatment and primary human endometrial epithelial cells share apical junctional complexes, interdigitations and even desmosomes at their lateral plasma membranes 24–48 h after confrontation in co-culture.

#### Hormonal control of junction expression

The changes in the cell–cell adhesion complexes are most likely brought about by the ovarian steroid hormones oestrogen and progesterone, which vary in their serum concentration during the menstrual cycle and in pregnancy. In cell culture, 17 $\beta$ -estradiol was found to enhance the motility of normal and neoplastic endometrial cells by rapid remodelling of the actin cytoskeleton and formation of focal adhesion complexes (Flamini et al. 2011). The direct influence of ovarian hormones on desmosomal proteins could be shown in rats (Preston et al. 2004). Progesterone treatment alone or in combination with estradiol administered to ovariectomised rats resulted in the same Dsg staining at the lateral membrane as in early pregnancy under physiological progesterone action. In the ovine uterus, progesterone administration stimulated a decline in tight junction and adherens junction-associated proteins in the endometrial luminal epithelium similar to the effects obtained in early pregnancy (Satterfield et al. 2007). Interestingly, a regulation of the endometrial WNT system by progesterone was reported for the ovine uterus by Satterfield et al. (2008). The authors proposed that specific WNT pathways alter tight and adherens junctions.

Fujimoto et al. (1998) suggested evidence for hormonal regulation of cell–cell adhesion in the human endometrium. The mRNA levels of E-cadherin,  $\alpha$ - and  $\beta$ -catenin were higher in the luteal phase than in the proliferative phase of the menstrual cycle. In addition, the mRNA levels of these proteins could be reduced again by treatment with

estradiol dipropionate. Although this is an interesting result, this study should be regarded with caution, since the data were obtained by semiquantitative Southern blot analysis of homogenised tissue samples and may only reflect the relative content of epithelial-to-stromal tissue.

In conclusion, the described alterations in cell–cell adhesion of human endometrial epithelial cells during the implantation window provide new *in vivo* data on the plasticity of cell–cell junctions and suggest a general change in endometrial epithelial cell morphology and polarity in preparation for trophoblast invasion under hormonal control. Further experimental studies *in vivo* on animal models and *in vitro* on human endometrial epithelial cells are required to prove this concept.

**Acknowledgments** Thanks are due to Dr. C. Krusche for useful comments and help with primer design and PCR protocol and to Diana Seelis-Schmidt, Claudia Schmitz and Vanessa Creutz for excellent technical assistance.

#### References

- Aplin JD, Charlton AK, Ayad S (1988) An immunohistochemical study of human endometrial extracellular matrix during the menstrual cycle and first trimester of pregnancy. *Cell Tissue Res* 253(1):231–240
- Bentin-Ley U, Horn T, Sjogren A, Sorensen S, Falck Larsen J, Hamberger L (2000) Ultrastructure of human blastocyst-endometrial interactions *in vitro*. *J Reprod Fertil* 120(2):337–350
- Bergh PA, Navot D (1992) The impact of embryonic development and endometrial maturity on the timing of implantation. *Fertil Steril* 58(3):537–542
- Bilalis DA, Klentzeris LD, Fleming S (1996) Immunohistochemical localization of extracellular matrix proteins in luteal phase endometrium of fertile and infertile patients. *Hum Reprod* 11(12):2713–2718
- Classen-Linke I, Denker HW (1990) Preparation of rabbit uterine epithelium for trophoblast attachment: histochemical changes in the apical and lateral membrane compartment. In: Denker HW, Aplin JD (eds) *Trophoblast Research*, vol 4. Plenum Medical Book Comp, New York and London, pp 307–322
- Cowin P, Kapprell HP, Franke WW, Tamkun J, Hynes RO (1986) Plakoglobin: a protein common to different kinds of intercellular adhering junctions. *Cell* 46(7):1063–1073
- Denker HW (1993) Implantation: a cell biological paradox. *J Exp Zool* 266(6):541–558
- Denker HW (1994) Endometrial receptivity: cell biological aspects of an unusual epithelium. A review *Ann Anat* 176(1):53–60
- Farquhar MG, Palade GE (1963) Junctional complexes in various epithelia. *J Cell Biol* 17:375–412
- Flamini MI, Sanchez AM, Genazzani AR, Simoncini T (2011) Estrogen regulates endometrial cell cytoskeletal remodeling and motility via focal adhesion kinase. *Fertil Steril* 95(2):722–726
- Fujimoto J, Ichigo S, Hori M, Tamaya T (1996) Alteration of E-cadherin, alpha- and beta-catenin mRNA expression in human uterine endometrium during the menstrual cycle. *Gynecol Endocrinol* 10(3):187–191
- Fujimoto J, Sakaguchi H, Hirose R, Tamaya T (1998) Significance of sex steroids in roles of cadherin subfamily and its related

- proteins in the uterine endometrium and placenta. *Horm Res* 50(Suppl 2):30–36
- Garrod D, Chidgey M (2008) Desmosome structure, composition and function. *Biochim Biophys Acta* 1778(3):572–587
- Holthofer B, Windoffer R, Troyanovsky S, Leube RE (2007) Structure and function of desmosomes. *Int Rev Cytol* 264:65–163
- Illingworth IM, Kiszka I, Bagley S, Ireland GW, Garrod DR, Kimber SJ (2000) Desmosomes are reduced in the mouse uterine luminal epithelium during the preimplantation period of pregnancy: a mechanism for facilitation of implantation. *Biol Reprod* 63(6):1764–1773
- Imai K, Maeda M, Fujiwara H, Kariya M, Takakura K, Kanzaki H, Mori T (1992) Dipeptidyl peptidase IV as a differentiation marker of the human endometrial glandular cells. *Hum Reprod* 7(9):1189–1194
- Kabir-Salmani M, Murphy CR, Hosseini A, Valojerdi MR (2008) Ultrastructural modifications of human endometrium during the window of implantation. *Int J Fertil Steril* 2(2):44–59
- Kametani Y, Takeichi M (2007) Basal-to-apical cadherin flow at cell junctions. *Nat Cell Biol* 9(1):92–98
- Martel D, Malet C, Gautray JP, Psychoyos A (1981) Surface changes of the luminal uterine epithelium during human menstrual cycle: a scanning electron microscopic study. In: de Brux J, Mortel R, Gautrey JP (eds) *The Endometrium: Hormonal Impacts*. Plenum Press, New York, pp 15–29
- Matsuzaki S, Darcha C, Maleysson E, Canis M, Mage G (2010) Impaired down-regulation of E-cadherin and beta-catenin protein expression in endometrial epithelial cells in the mid-secretory endometrium of infertile patients with endometriosis. *J Clin Endocrinol Metab* 95(7):3437–3445
- Morris K, Ihnatovych I, Ionetz E, Reed J, Braundmeier A, Strakova Z (2011) Cofilin and slingshot localization in the epithelium of uterine endometrium changes during the menstrual cycle and in endometriosis. *Reprod Sci* 18(10):1014–1024
- Moser G, Gauster M, Orendi K, Glasner A, Theuerkauf R, Huppertz B (2010) Endoglandular trophoblast, an alternative route of trophoblast invasion? Analysis with novel confrontation co-culture models. *Hum Reprod* 25(5):1127–1136
- Murphy CR, Swift JG, Need JA, Mukherjee TM, Rogers AW (1982) A freeze-fracture electron microscopic study of tight junctions of epithelial cells in the human uterus. *Anat Embryol (Berl)* 163(4):367–370
- Murphy CR, Rogers PA, Hosie MJ, Leeton J, Beaton L (1992) Tight junctions of human uterine epithelial cells change during the menstrual cycle: a morphometric study. *Acta Anat (Basel)* 144(1):36–38
- Nei H, Saito T, Tobioka H, Itoh E, Mori M, Kudo R (1996) Expression of component desmosomal proteins in uterine endometrial carcinoma and their relation to cellular differentiation. *Cancer* 78(3):461–470
- Nikas G, Drakakis P, Loutradis D, Mara-Skoufari C, Koumantakis E, Michalakis S, Psychoyos A (1995) Uterine pinopodes as markers of the ‘nidation window’ in cycling women receiving exogenous oestradiol and progesterone. *Hum Reprod* 10(5):1208–1213
- Noyes RW, Hertig AT, Rock J (1950) Dating the endometrial biopsy. *Fertil Steril* 1(1):3–25
- Preston AM, Lindsay LA, Murphy CR (2004) Progesterone treatment and the progress of early pregnancy reduce desmoglein 1&2 staining along the lateral plasma membrane in rat uterine epithelial cells. *Acta Histochem* 106(5):345–35110
- Preston AM, Lindsay LA, Murphy CR (2006) Desmosomes in uterine epithelial cells decrease at the time of implantation: an ultrastructural and morphometric study. *J Morphol* 267(1):103–108
- Roberts BJ, Pashaj A, Johnson KR, Wahl JK 3rd (2011) Desmosome dynamics in migrating epithelial cells requires the actin cytoskeleton. *Exp Cell Res* 317(20):2814–2822
- Sarani SA, Ghaffari-Novin M, Warren MA, Dockery P, Cooke ID (1999) Morphological evidence for the ‘implantation window’ in human luminal endometrium. *Hum Reprod* 14(12):3101–3106
- Satterfield MC, Dunlap KA, Hayashi K, Burghardt RC, Spencer TE, Bazer FW (2007) Tight and adherens junctions in the ovine uterus: differential regulation by pregnancy and progesterone. *Endocrinology* 148(8):3922–3931
- Satterfield MC, Song G, Hayashi K, Bazer FW, Spencer TE (2008) Progesterone regulation of the endometrial WNT system in the ovine uterus. *Reprod Fertil Dev* 20(8):935–946
- Schlafke S, Enders AC (1975) Cellular basis of interaction between trophoblast and uterus at implantation. *Biol Reprod* 12(1):41–65
- Schlegel N, Meir M, Heupel WM, Holthofer B, Leube RE, Waschke J (2010) Desmoglein 2-mediated adhesion is required for intestinal epithelial barrier integrity. *Am J Physiol Gastrointest Liver Physiol* 298(5):G774–G783
- Schroeder A, Mueller O, Stocker S, Salowsky R, Leiber M, Gassmann M, Lightfoot S, Menzel W, Granzow M, Ragg T (2006) The RIN: an RNA integrity number for assigning integrity values to RNA measurements. *BMC Mol Biol* 7:3
- Suzuki M, Kuramoto H, Izumi S, Shirane H, Watanabe K (1981) Cyclic changes of alkaline-phosphatase in the human endometrium - histochemical and biochemical analysis. *Acta Histochem Cytochem* 14(5):524–533
- Tabibzadeh S, Babaknia A, Kong QF, Zupi E, Marconi D, Romanini C, Satyaswaroop PG (1995) Menstruation is associated with disordered expression of desmoplakin I/II and cadherin/catenins and conversion of F- to G-actin in endometrial epithelium. *Hum Reprod* 10(4):776–784
- Tanaka T, Wang C, Umesaki N (2009) Remodeling of the human endometrial epithelium is regulated by laminin and type IV collagen. *Int J Mol Med* 23(2):173–180
- Thie M, Fuchs P, Denker HW (1996) Epithelial cell polarity and embryo implantation in mammals. *Int J Dev Biol* 40(1):389–393
- Winterhager E, Kuhnel W (1982) Alterations in intercellular junctions of the uterine epithelium during the preimplantation phase in the rabbit. *Cell Tissue Res* 224(3):517–526